Theory of intrapolymer excimer-formation kinetics

Jaeyoung Sung,[a] Jinuk Lee, and Sangyoub Lee[b]
School of Chemistry and Molecular Engineering, and Center for Molecular Catalysis, Seoul National University, Seoul 151-747, South Korea

(Received 28 August 2002; accepted 7 October 2002)

We generalize the Wilemski–Fixman theory for reversible polymer cyclization to treat the kinetics of intrachain excimer-formation reactions. While most previous theories for intrachain reactions dealt with the end-to-end reaction case, we consider the general situation in which the reacting groups are located at any place on the chain backbone. Various aspects of the reaction kinetics, such as the effect of hydrodynamic interaction and the dependence of reaction rate on the positions of reacting groups as well as on the chain length, are investigated. © *2003 American Institute of Physics.* [DOI: 10.1063/1.1525801]

I. INTRODUCTION

Much attention has been paid to the intrachain reactions of polymers because such reactions occur in a variety of reacting polymer systems and measurements of the intrachain reaction rates provide valuable information on the conformational structure and dynamical behavior of polymer chains.[1,2]

A general theory for describing the diffusion-influenced kinetics of intrachain reactions was first advanced by Wilemski and Fixman.[3] By utilizing a factorization approximation (also called the closure approximation), they could derive analytic expressions for the reaction rate and the time-dependent survival probability of unreacted polymer for several types of intrachain reactions. The accuracy of the Wilemski–Fixman (WF) theory has been assessed by several authors. Doi derived a variational principle for the asymptotic rate constant, and showed that use of the simplest trial function reproduces the WF result.[4] Battezzati and Perico[5] and Weiss[6] carried out systematic perturbation analyses to examine the validity of the WF theory. In particular, Weiss clearly showed that the WF theory can be reproduced by making a Padé approximation to the perturbation series involving multiple integrals. This aspect has also been pointed out by Seki, Barzykin, and Tachiya,[7] who utilized a projection operator approach. Recently, several groups have carried out Brownian dynamics simulations to assess the accuracy of the WF theory.[8–10] They found that the closure approximation may yield an inaccurate result when the range of the reaction sink is larger than the polymer mean bond length.

More specific aspects of the intrachain reactions have been investigated also. Friedman and O'Shaughnessy developed a renormalization group method for calculating the cyclization rates of chain polymers as a function of reactive group locations along the backbone.[11] Stampe and Sokolov investigated the effects of electrostatic interaction between the charged end groups on the cyclization rate.[12] Dua and Cherayil considered the effect of backbone rigidity on the dynamics of chain closure.[13] Bandyopadhyay and Ghosh utilized a non-Markovian reaction-diffusion equation to investigate the memory effect in the fluorescence resonance energy transfer.[14] Rey and Freire,[15] and more recently Podtelezhnikov and Vologodskii,[16] investigated the effect of excluded volume interactions by using Brownian dynamics simulations.

In the present work, we consider the kinetics of a reversible excimer-formation reaction occurring in a chain polymer. As depicted in Fig. 1, we treat the general case in which the reacting groups are located at any place of the chain. When the lifetimes of the monomer and excimer are set equal to infinity, the reaction model reduces to that for reversible polymer cyclization, which was considered by Wilemski and Fixman.[3] As already noted by them, the WF theory does not predict the correct asymptotic relaxation kinetics as the reaction system is restored to equilibrium. We show how this problem can be solved in the framework of the present theory.

In Sec. II, we formulate the theory. The key dynamic quantity in the formalism is the reduced Green's function which describes the relative dynamics of the reacting groups. In Sec. III, we present an explicit expression for the Green's function that varies with the positions of reacting groups along the chain backbone and which also includes the effect of hydrodynamic interaction. In Sec. IV, we then discuss some key aspects of the excimer-formation kinetics that are revealed by the present theory, and conclude our work in Sec. V.

II. DERIVATION OF THE RATE EXPRESSIONS

A. Excimer-formation kinetics

Let $\psi_O(\mathbf{r}^{N+1},t)$ be the probability density that the polymer is in the open form with an electronically excited monomer at time t, and that $N+1$ beads constituting the chain located at $\mathbf{r}^{N+1}\equiv(\mathbf{r}_0,\mathbf{r}_1,\ldots,\mathbf{r}_N)$. Similarly, $\psi_R(\mathbf{x}^{N+1},t)$ is the probability density for the polymer making a ring due to the formation of an excimer, with the $N+1$ beads located at $\mathbf{x}^{N+1}\equiv(\mathbf{x}_0,\mathbf{x}_1,\ldots,\mathbf{x}_N)$. The probability density function $\psi_O(\mathbf{r}^{N+1},t)$ evolves in time according to[3]

[a]Present address: Department of Chemistry and Center for Materials Science and Engineering, Massachusetts Institute of Technology, Cambridge, MA 02139.
[b]Electronic mail: snagyoub@snu.ac.kr

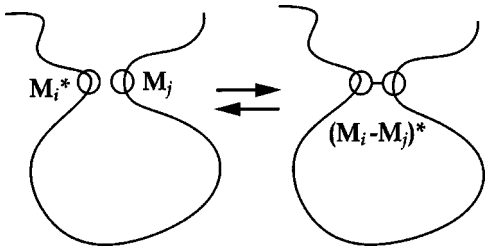

FIG. 1. Pictorial representation of the intrapolymer excimer-formation reaction under consideration.

$$\frac{\partial}{\partial t}\psi_O(\mathbf{r}^{N+1},t)=\mathcal{L}(\mathbf{r}^{N+1})\psi_O(\mathbf{r}^{N+1},t)-k_M\psi_O(\mathbf{r}^{N+1},t)-\int d\mathbf{x}^{N+1}R_f(\mathbf{r}^{N+1}|\mathbf{x}^{N+1})\psi_O(\mathbf{r}^{N+1},t)+\int d\mathbf{x}^{N+1}R_r(\mathbf{x}^{N+1}|\mathbf{r}^{N+1})\psi_R(\mathbf{x}^{N+1},t). \tag{2.1}$$

Here $\mathcal{L}(\mathbf{r}^{N+1})$ is the Smoluchowki operator governing the thermal evolution of the open-chain distribution in the absence of reaction, and k_M denotes the decay rate constant of the excited monomer. The sink functions R_f and R_r represent the inherent rates of excimer formation and dissociation at the bead configurations given by $\mathbf{r}^{N+1}$ and $\mathbf{x}^{N+1}$, respectively. We assume that they have the simple forms given by

$$R_f(\mathbf{r}^{N+1}|\mathbf{x}^{N+1})=S_f^0(\mathbf{r}^{N+1})\,\delta(\mathbf{r}^{N+1}-\mathbf{x}^{N+1}),\qquad R_r(\mathbf{x}^{N+1}|\mathbf{r}^{N+1})=S_r^0(\mathbf{x}^{N+1})\,\delta(\mathbf{r}^{N+1}-\mathbf{x}^{N+1}), \tag{2.2}$$

where $\delta(\mathbf{r}^{N+1}-\mathbf{x}^{N+1})=\delta(\mathbf{r}_0-\mathbf{x}_0)\cdots\delta(\mathbf{r}_N-\mathbf{x}_N)$. Equation (2.2) tells us that the inherent bond formation and dissociation occur so rapidly that the polymer conformation does not change much during the course of the reactive transitions. With Eq. (2.2), Eq. (2.1) reduces to

$$\frac{\partial}{\partial t}\psi_O(\mathbf{r}^{N+1},t)=\mathcal{L}(\mathbf{r}^{N+1})\psi_O(\mathbf{r}^{N+1},t)-k_M\psi_O(\mathbf{r}^{N+1},t)-S_f^0(\mathbf{r}^{N+1})\psi_O(\mathbf{r}^{N+1},t)+S_r^0(\mathbf{r}^{N+1})\psi_R(\mathbf{r}^{N+1},t). \tag{2.3}$$

We now suppose that the reacting groups are located at the ith and jth beads, and thus assume the following sink functions:

$$S_f^0(\mathbf{r}^{N+1})=\kappa_f S_f(|\mathbf{r}_i-\mathbf{r}_j|), \tag{2.4}$$

$$S_r^0(\mathbf{r}^{N+1})=\kappa_r S_r(|\mathbf{r}_i-\mathbf{r}_j|). \tag{2.5}$$

With these sink functions, integration of Eq. (2.1) over $(\mathbf{r}_0,\ldots,\mathbf{r}_{i-1},\mathbf{r}_{i+1},\ldots,\mathbf{r}_{j-1},\mathbf{r}_{j+1},\ldots,\mathbf{r}_N)$ gives

$$\frac{\partial}{\partial t}P_O'(\mathbf{r}_i,\mathbf{r}_j,t)=L'(\mathbf{r}_i,\mathbf{r}_j)P_O'(\mathbf{r}_i,\mathbf{r}_j,t)-k_MP_O'(\mathbf{r}_i,\mathbf{r}_j,t)-\kappa_f S_f(|\mathbf{r}_i-\mathbf{r}_j|)P_O'(\mathbf{r}_i,\mathbf{r}_j,t)+\kappa_r S_r(|\mathbf{r}_i-\mathbf{r}_j|)P_R'(\mathbf{r}_i,\mathbf{r}_j,t). \tag{2.6}$$

$P_O'(\mathbf{r}_i,\mathbf{r}_j,t)\,[P_R'(\mathbf{r}_i,\mathbf{r}_j,t)]$ is the probability density that the polymer is in the open [ring] form at time t and that the ith and jth beads at $\mathbf{r}_i$ and $\mathbf{r}_j$. $L'(\mathbf{r}_i,\mathbf{r}_j)$ is the reduced Smoluchowski operator governing the thermal evolution of $P_O'(\mathbf{r}_i,\mathbf{r}_j,t)$ in the absence of a reaction. When the external flows and forces are absent, it is clear that $P_O'(\mathbf{r}_i,\mathbf{r}_j,t)$ and $P_R'(\mathbf{r}_i,\mathbf{r}_j,t)$ depend only on $R(\equiv|\mathbf{r}_i-\mathbf{r}_j|)$:

$$P_O'(\mathbf{r}_i,\mathbf{r}_j,t)=V^{-1}P_O(R,t),\qquad P_R'(\mathbf{r}_i,\mathbf{r}_j,t)=V^{-1}P_R(R,t). \tag{2.7}$$

$P_O(R,t)\,[P_R(R,t)]$ is the probability density that the polymer is in the open [ring] form at time t and that the distance between the ith and jth beads is given by R. Hence, Eq. (2.6) reduces to

$$\frac{\partial}{\partial t}P_O(R,t)=L(R)P_O(R,t)-k_MP_O(R,t)-\kappa_f S_f(R)P_O(R,t)+\kappa_r S_r(R)P_R(R,t). \tag{2.8}$$

Here, $L(R)$ is an effective thermal operator governing the reaction-free evolution of $P_O(R,t)$, whose explicit expression need not be known at the moment.

If the vibration of the excimer-forming bond is very fast, the deviation of $P_R(R,t)$ from the internal equilibrium distribution $P_R^{\mathrm{eq}}(R)$ should be negligible, so that we can write

$$P_R(R,t)\cong P_R^{\mathrm{eq}}(R)S_R(t). \tag{2.9}$$

$S_R(t)$ is the probability that the polymer is in the ring form at time t. With this approximation, Eq. (2.8) can be rewritten as

$$\frac{\partial}{\partial t}P_O(R,t)=L(R)P_O(R,t)-k_MP_O(R,t)-\kappa_f S_f(R)P_O(R,t)+\kappa_r S_r(R)P_R^{\mathrm{eq}}(R)S_R(t). \tag{2.10}$$

Integrating Eq. (2.10) over $\mathbf{R}$ (i.e., over the relative separation and orientation of the ith and jth beads), we obtain the rate equation as

$$\frac{d}{dt}S_O(t)=-k_MS_O(t)-\kappa_f\int d\mathbf{R}\,S_f(R)P_O(R,t)+k_r^{\mathrm{eq}}S_R(t). \tag{2.11}$$

Here $S_O(t)$ is the probability that the polymer is in the open form at time t, and k_r^{eq} denotes the equilibrium rate constant for the excimer-dissociation:

$$S_O(t)=\int d\mathbf{R}\,P_O(R,t), \tag{2.12}$$

$$k_r^{\mathrm{eq}}=\kappa_r\int d\mathbf{R}\,S_r(R)P_R^{\mathrm{eq}}(R). \tag{2.13}$$

When the lifetime of the excimer is different from that of the excited monomer, we need an additional rate equation for $S_R(t)$ given by

$$\frac{d}{dt}S_R(t) = -k_E S_R(t) + \kappa_f \int d\mathbf{R}\, S_f(R) P_O(R,t) - k_r^{\mathrm{eq}} S_R(t), \tag{2.14}$$

where k_E denotes the decay rate constant of the excimer. The key reaction dynamic quantities $S_O(t)$ and $S_R(t)$ can be determined by solving the set of equations given by Eqs. (2.10), (2.11), and (2.14).

We assume that initially the polymer is in the equilibrium configuration of the open chain with a monomer just excited:

$$S_O(t=0) = 1,\ P_O(R,t=0) = P_O^{\mathrm{eq}}(R). \tag{2.15}$$

For this initial condition, Laplace transformation of Eq. (2.10) yields the following perturbative solution:

$$\begin{aligned}\int d\mathbf{R}\, S_f(R)\hat{P}_O(R,s) &= s_M^{-1}\int d\mathbf{R}\, S_f(R) P_O^{\mathrm{eq}}(R) \\ &- \kappa_f s_M^{-1}\Big\{\int d\mathbf{R}\, S_f(R)\int d\mathbf{R}_0 \hat{G}(R,s_M|R_0) S_f(R_0) P_O^{\mathrm{eq}}(R_0) \\ &- \kappa_f \int d\mathbf{R}\, S_f(R)\int d\mathbf{R}_1 \hat{G}(R,s_M|R_1) S_f(R_1)\int d\mathbf{R}_0 \hat{G}(R_1,s_M|R_0) S_f(R_0) P_O^{\mathrm{eq}}(R_0) + \cdots\Big\} \\ &+ \kappa_r \hat{S}_R(s)\Big\{\int d\mathbf{R}\, S_f(R)\int d\mathbf{R}_0 \hat{G}(R,s_M|R_0) S_r(R_0) P_R^{\mathrm{eq}}(R_0) \\ &- \kappa_f \int d\mathbf{R}\, S_f(R)\int d\mathbf{R}_1 \hat{G}(R,s_M|R_1) S_f(R_1)\int d\mathbf{R}_0 \hat{G}(R_1,s_M|R_0) S_r(R_0) P_R^{\mathrm{eq}}(R_0) + \cdots\Big\}. \end{aligned} \tag{2.16}$$

We denote the Laplace transform of any function $f(t)$ as $\hat{f}(s)$. In Eq. (2.16), $s_M = s + k_M$, and the Green's function $\hat{G}(R,s|R_0)$ is defined by

$$\hat{G}(R,s|R_0) = \frac{1}{s - L(R)}\,\frac{\delta(R-R_0)}{4\pi R_0^2}. \tag{2.17}$$

By using the decoupling approximation suggested by Weiss,[6] we can resum the series solution in Eq. (2.16) as

$$\begin{aligned}\int d\mathbf{R}\, S_f(R)\hat{P}_O(R,s) &\cong \frac{v_f}{s_M} - \frac{\kappa_f}{s_M}\cdot\frac{\hat{D}_f(s_M)}{1+\kappa_f\hat{D}_f(s_M)/v_f} \\ &+ \kappa_r \hat{S}_R(s)\,\frac{\hat{D}_r(s_M)}{1+\kappa_f\hat{D}_f(s_M)/v_f}, \end{aligned} \tag{2.18}$$

where

$$v_f = \int d\mathbf{R}\, S_f(R) P_O^{\mathrm{eq}}(R), \tag{2.19}$$

$$D_f(t) = \int d\mathbf{R}\, S_f(R)\int d\mathbf{R}_0 G(R,t|R_0) S_f(R_0) P_O^{\mathrm{eq}}(R_0), \tag{2.20}$$

$$D_r(t) = \int d\mathbf{R}\, S_f(R)\int d\mathbf{R}_0 G(R,t|R_0) S_r(R_0) P_R^{\mathrm{eq}}(R_0). \tag{2.21}$$

On the other hand, Laplace transformation of Eqs. (2.11) and (2.14) gives

$$\begin{aligned}&\kappa_f\int d\mathbf{R}\, S_f(R)\hat{P}_O(R,s) - k_r^{\mathrm{eq}}\hat{S}_R(s) \\ &= (s+k_E)\hat{S}_R(s) = 1-(s+k_M)\hat{S}_O(s). \end{aligned} \tag{2.22}$$

Substitution of Eq. (2.18) into Eq. (2.22) finally gives

$$\begin{aligned}\hat{S}_R(s) = \frac{k_f^{\mathrm{eq}}}{s+k_M}\Bigg\{(s+k_E)\Bigg[1+k_f^{\mathrm{eq}}\frac{\hat{D}_f(s+k_M)}{D_f(\infty)}\Bigg] + k_r^{\mathrm{eq}} \\ + k_f^{\mathrm{eq}}k_r^{\mathrm{eq}}\Bigg[\frac{\hat{D}_f(s+k_M)}{D_f(\infty)} - \frac{\hat{D}_r(s+k_M)}{D_r(\infty)}\Bigg]\Bigg\}^{-1}, \end{aligned} \tag{2.23}$$

$$\hat{S}_O(s) = (s+k_M)^{-1}[1-(s+k_E)\hat{S}_R(s)], \tag{2.24}$$

where

$$k_f^{\mathrm{eq}} = \kappa_f \int d\mathbf{R}\, S_f(R) P_O^{\mathrm{eq}}(R) = \kappa_f v_f. \tag{2.25}$$

Note that $D_f(\infty) = v_f^2$ and $D_r(\infty) = v_f \int d\mathbf{R}\, S_r(R) P_R^{\mathrm{eq}}(R)$. Equations (2.23) and (2.24) are the key results of the formalism developed in this section.

When the sink functions can be modeled as δ functions [*i.e.*, when $S_f(R) = S_r(R) = \delta(R-\sigma)/(4\pi\sigma^2)$], Eq. (2.23) reduces to

$$\hat{S}_R(s) = \frac{k_f^{\mathrm{eq}}}{(s+k_M)(s+k_E)[1+\kappa_f\hat{G}(\sigma,s+k_M|\sigma) + (s+k_E)^{-1}k_r^{\mathrm{eq}}]}. \tag{2.26}$$

It should be remarked that the decoupling approximation of Weiss becomes exact in this δ-function sink case.

B. Reversible cyclization kinetics

When $k_M = k_E = 0$, the present problem reduces to that of reversible polymer cyclization, which was first considered by Wilemski and Fixman.[3] In this special case, Eq. (2.23) reduces to

$$\hat{S}_R(s) = \frac{k_f^{\mathrm{eq}}}{s}\left\{ s + k_f^{\mathrm{eq}} \frac{s\hat{D}_f(s)}{D_f(\infty)} + k_r^{\mathrm{eq}} + k_f^{\mathrm{eq}} k_r^{\mathrm{eq}} \left[\frac{\hat{D}_f(s)}{D_f(\infty)} - \frac{\hat{D}_r(s)}{D_r(\infty)} \right] \right\}^{-1}. \tag{2.27}$$

This can be compared with the WF result:

$$\hat{S}_R^{\mathrm{WF}}(s) = \frac{k_f^{\mathrm{eq}}}{s}\left\{ s + k_f^{\mathrm{eq}} \frac{s\hat{D}_f(s)}{D_f(\infty)} + k_r^{\mathrm{eq}} + k_f^{\mathrm{eq}} k_r^{\mathrm{eq}} \left[\frac{\hat{D}_f(s)}{D_f(\infty)} - \nu_f^{-1}\hat{R}(s) \right] \right\}^{-1} \tag{2.28}$$

with

$$R(t) = \int d\mathbf{R}\, S_f(R) \int d\mathbf{R}_0 G(R,t|R_0) P_R^{\mathrm{eq}}(R_0).$$

At long times, when the equilibrium state is restored, we should have

$$\lim_{t\to\infty} S_R(t) = \lim_{s\to 0} s\hat{S}_R(s) = \frac{k_f^{\mathrm{eq}}}{k_f^{\mathrm{eq}} + k_r^{\mathrm{eq}}} \equiv S_R^{\mathrm{eq}}. \tag{2.29}$$

However, neither of the solutions given by Eqs. (2.27) and (2.28) satisfies this requirement in general. We can remedy this problem immediately. When the system is restored to the equilibrium state, we should have $P_O(R,t) = P_O^{\mathrm{eq}}(R) S_O^{\mathrm{eq}}$ and Eq. (2.10) reduces to

$$\kappa_f S_f(R) P_O^{\mathrm{eq}}(R) S_O^{\mathrm{eq}} = \kappa_r S_r(R) P_R^{\mathrm{eq}}(R) S_R^{\mathrm{eq}}. \tag{2.30}$$

With this detailed balance condition, Eq. (2.27) becomes

$$\hat{S}_R(s) = \frac{k_f^{\mathrm{eq}}}{s}\left\{ s + k_f^{\mathrm{eq}} \frac{s\hat{D}_f(s)}{D_f(\infty)} + k_r^{\mathrm{eq}} \right\}^{-1}. \tag{2.31}$$

One can immediately see that Eq. (2.31) satisfies the equilibrium condition given by Eq. (2.29).

In contrast, the WF solution cannot be saved by the above detailed balance condition. The reason is that in the WF theory a couple of approximations were made at the stage of Eq. (2.3). First, $S_r^0(\mathbf{r}^{N+1})$ was set equal to a constant k_r. Second, $\psi_R(\mathbf{r}^{N+1},t)$ was approximated by $\psi_R^{\mathrm{eq}}(\mathbf{r}^{N+1}) S_R(t)$, where $\psi_R^{\mathrm{eq}}(\mathbf{r}^{N+1})$ is the equilibrium chain distribution function for the ring polymer. Thus, one can easily see that the WF solution is regained from our solution if $S_r(R)$ is set equal to unity.

In the special case when $S_f(R) = S_r(R) = \delta(R-\sigma)/(4\pi\sigma^2)$, Eq. (2.31) reduces to

$$\hat{S}_R(s) = \frac{1}{s} \cdot \frac{k_f^{\mathrm{eq}}}{s + \kappa_f s\hat{G}(\sigma,s|\sigma) + k_r^{\mathrm{eq}}}. \tag{2.32}$$

This equation can also be obtained from Eq. (2.26).

III. DERIVATION OF THE GREEN'S FUNCTION

To calculate the intrachain reaction rate between two reactive groups on a polymer, we need an explicit Green's function expression for the relative motion of the beads carrying the groups.

To the best of our knowledge, only the Green's function for the end-to-end motion of a polymeric chain has been given in the literature. For the free draining Rouse chain, the following expression has been derived by Wilemski and Fixman[3] using the boson representation method and also by Doi[17] using the more straightforward integration procedure:

$$G(\mathbf{R},t|\mathbf{R}_0) = \left(\frac{3}{2\pi L^2[1-\phi^2(t)]} \right)^{3/2} \times \exp\left\{ -\frac{3}{2L^2} \frac{[\mathbf{R} - \phi(t)\mathbf{R}_0]^2}{[1-\phi^2(t)]} \right\}. \tag{3.1}$$

Here, $\mathbf{R}$ is the end-to-end vector $\mathbf{r}_0 - \mathbf{r}_N$, and $L^2 (= Nb^2)$ is the equilibrium mean squared end-to-end distance with b^2 denoting the equilibrium mean squared length of a single bond of the Rouse chain. $\phi(t)$ is given by

$$\phi(t) = \frac{8}{\pi^2} \sum_{\mathrm{odd}\,k} \frac{1}{k^2} \exp(-3\lambda_k^o t/t_1),$$

$$\lambda_k^o = \left(\frac{k\pi}{N} \right)^2 \quad (k = 0,1,\ldots,N), \tag{3.2}$$

where t_1 is the characteristic diffusion time scale defined by $t_1 \equiv b^2/D_1$, and D_1 is the diffusion constant of a single bead. The expression for $\phi(t)$ given in Eq. (3.2) is valid only for large N. A more accurate expression for $\phi(t)$ is[8,18]

$$\phi(t) = \frac{8}{N(N+1)} \sum_{\mathrm{odd}\,k} \left(\frac{1}{\lambda_k^R} - \frac{1}{4} \right) \exp(-3\lambda_k^R t/t_1), \tag{3.3}$$

where $\lambda_k^R (k = 0,1,\ldots,N)$ is the Rouse eigenvalue given by

$$\lambda_k^R = 4\sin^2\left(\frac{k\pi}{2(N+1)} \right). \tag{3.4}$$

Note that in Eqs. (3.2) and (3.3) summation includes only the odd values of k.

We will now derive a more general expression for $G(\mathbf{R},t|\mathbf{R}_0)$ with $\mathbf{R} = \mathbf{r}_i - \mathbf{r}_j (0 \leqslant i < j \leqslant N)$. To simplify the analysis, we consider a Rouse–Zimm chain[19] with $N+1$ beads and neglect the excluded volume interactions. Let $\psi(\mathbf{r}^{N+1},t)$ be the probability density function that the $N+1$ beads are located at $\mathbf{r}^{N+1} \equiv (\mathbf{r}_0, \mathbf{r}_1, \ldots, \mathbf{r}_N)$ at time t. In the Rouse–Zimm model, the potential energy of the chain is given by

$$U/k_BT = \frac{3}{2b^2} \sum_{i=1}^{N} (\mathbf{r}_i - \mathbf{r}_{i-1})^2 = \frac{3}{2b^2} \sum_{\gamma=x,y,z} \mathbf{X}_\gamma^T \cdot \mathbf{A} \cdot \mathbf{X}_\gamma, \tag{3.5}$$

where $\mathbf{A}$ is the $(N+1)\times(N+1)$ matrix given by

$$\mathbf{A}=\begin{pmatrix} 1 & -1 & 0 & 0 & \cdots & 0 & 0 & 0 \\ -1 & 2 & -1 & 0 & \cdots & 0 & 0 & 0 \\ 0 & -1 & 2 & -1 & \cdots & 0 & 0 & 0 \\ 0 & 0 & -1 & 2 & \cdots & 0 & 0 & 0 \\ \vdots & \vdots & \vdots & \vdots & \ddots & \vdots & \vdots & \vdots \\ 0 & 0 & 0 & 0 & \cdots & 2 & -1 & 0 \\ 0 & 0 & 0 & 0 & \cdots & -1 & 2 & -1 \\ 0 & 0 & 0 & 0 & \cdots & 0 & -1 & 1 \end{pmatrix}$$

and $\mathbf{X}_\gamma$ is the $(N+1)$ -dimensional vector defined by

$$\mathbf{X}_x=\begin{pmatrix} x_0 \\ x_1 \\ \vdots \\ x_N \end{pmatrix}, \quad \mathbf{X}_y=\begin{pmatrix} y_0 \\ y_1 \\ \vdots \\ y_N \end{pmatrix}, \quad \mathbf{X}_z=\begin{pmatrix} z_0 \\ z_1 \\ \vdots \\ z_N \end{pmatrix}$$

with the superscript T denoting the transpose. The hydrodynamic coupling between the beads is taken into account in a preaveraged form, and the evolution equation for $\psi(\mathbf{r}^{N+1},t)$ in the absence of reaction is given by

$$\frac{\partial\psi}{\partial t}=D_1\sum_{\gamma=x,y,z}\left[\left(\frac{\partial}{\partial\mathbf{X}_\gamma}\right)^T\cdot\mathbf{H}\cdot\left(\frac{\partial\psi}{\partial\mathbf{X}_\gamma}\right)+\frac{3}{b^2}\left(\frac{\partial}{\partial\mathbf{X}_\gamma}\right)^T\cdot\mathbf{H}\cdot\mathbf{A}\cdot\mathbf{X}_\gamma\psi\right]. \tag{3.6}$$

$\mathbf{H}$ is the matrix describing the preaveraged hydrodynamic interaction between the beads that is given by

$$H_{ij}=\begin{cases} 1 & (i=j) \\ \dfrac{\zeta_1}{\eta b(6\pi^3|i-j|)^{1/2}} & (i\neq j) \end{cases},$$

where $\zeta_1(=k_BT/D_1)$ denotes the friction coefficient for a single bead, and η is the solvent viscosity.

Let $\mathbf{Q}$ denote a matrix whose $N+1$ columns are the eigenvectors of the matrix $\mathbf{H}\cdot\mathbf{A}$, so that $\mathbf{H}\cdot\mathbf{A}$ is diagonalized by the similarity transformation:

$$\mathbf{Q}^{-1}\cdot\mathbf{H}\cdot\mathbf{A}\cdot\mathbf{Q}=\mathbf{\Lambda}$$

with

$$\Lambda_{ij}=\lambda_i\delta_{ij}. \tag{3.7}$$

Zimm showed that the same matrix $\mathbf{Q}$ can also be used to diagonalize $\mathbf{H}$ and $\mathbf{A}$ separately, though not by similarity transformations,

$$\mathbf{Q}^T\cdot\mathbf{A}\cdot\mathbf{Q}=\mathbf{M}$$

with

$$M_{ij}=\mu_i\delta_{ij}, \tag{3.8}$$
$$\mathbf{Q}^{-1}\cdot\mathbf{H}\cdot\mathbf{Q}^{-1T}=\mathbf{\Lambda}\cdot\mathbf{M}^{-1}=\mathbf{N}$$

with

$$N_{ij}=\nu_i\delta_{ij}=(\lambda_i/\mu_i)\delta_{ij}. \tag{3.9}$$

Hence by introducing the normal coordinates $\{\mathbf{q}_k=(q_{kx},q_{ky},q_{kz})\}$ defined by

$$\mathbf{r}_i=\sum_{k=0}^{N}Q_{ik}\mathbf{q}_k, \tag{3.10}$$

Eq. (3.6) can be rewritten as

$$\frac{\partial}{\partial t}\psi(\mathbf{q}^{N+1},t)=D_1\sum_{i=0}^{N}\nu_i\left[\frac{\partial^2\psi}{\partial\mathbf{q}_i^2}+2\alpha_i\left(\frac{\partial}{\partial\mathbf{q}_i}\right)^T\cdot\mathbf{q}_i\psi\right], \tag{3.11}$$

where $\alpha_i=(3\mu_i)/(2b^2)$ and $\mathbf{q}^{N+1}=(\mathbf{q}_0,\mathbf{q}_1,\ldots,\mathbf{q}_N)$. Except for $\mathbf{q}_0$ corresponding to the center-of-mass motion, the normal modes are overdamped harmonic oscillators with force constants $2\alpha_ik_BT$ and diffusion constants $D_1\nu_i$.

From Eq. (3.10), we have

$$\mathbf{R}=\mathbf{r}_i-\mathbf{r}_j=\sum_{k=0}^{N}c_k\mathbf{q}_k \tag{3.12}$$

with $c_k=Q_{ik}-Q_{jk}$. Note that $c_0=0$ since $\mathbf{R}$ should be independent of the center-of-mass coordinates. Hence the Green's function $G(\mathbf{R},t|\mathbf{R}_0)$ can be expressed as

$$G(\mathbf{R},t|\mathbf{R}_0)=\mathcal{N}\int d\mathbf{q}^{N+1}\int d\mathbf{q}_0^{N+1}\delta\left(\sum_{i=1}^{N}c_i\mathbf{q}_i-\mathbf{R}\right)\times\mathcal{G}_F(\mathbf{q}^{N+1},t|\mathbf{q}_0^{N+1})\times\delta\left(\sum_{j=1}^{N}c_j\mathbf{q}_{j0}-\mathbf{R}_0\right)\psi_{\mathrm{eq}}(\mathbf{q}_0^{N+1}). \tag{3.13}$$

Here, $\mathcal{G}_F(\mathbf{q}^{N+1},t|\mathbf{q}_0^{N+1})$ is the full Green's function for Eq. (3.11) satisfying the initial condition,

$$\mathcal{G}_F(\mathbf{q}^{N+1},t=0|\mathbf{q}_0^{N+1})=\prod_{i=0}^{N}\delta(\mathbf{q}_i-\mathbf{q}_{i0}).$$

$\psi_{\mathrm{eq}}(\mathbf{q}^{N+1})$ is the equilibrium distribution function, and $\mathcal{N}$ is the normalization constant, whose expressions are derived in the following.

First, $\psi_{\mathrm{eq}}(\mathbf{q}^{N+1})$ can be obtained easily by solving

$$\sum_{i=0}^{N}\nu_i\left[\frac{\partial^2\psi_{\mathrm{eq}}}{\partial\mathbf{q}_i^2}+2\alpha_i\left(\frac{\partial}{\partial\mathbf{q}_i}\right)^T\cdot\mathbf{q}_i\psi_{\mathrm{eq}}\right]=0. \tag{3.14}$$

We have

$$\psi_{\mathrm{eq}}(\mathrm{q}^{N+1})=V^{-1}\prod_{i=1}^{N}(\alpha_i/\pi)^{3/2}\exp(-\alpha_i\mathbf{q}_i^2), \tag{3.15}$$

where V is the volume of the system. The normalization constant $\mathcal{N}$ appearing in Eq. (3.13) is obtained by requiring that $\int d\mathbf{R}\,G(\mathbf{R},t|\mathbf{R}_0)=1$. For $t=0$, this requirement on Eq. (3.13) gives

$$\mathcal{N}\int d\mathbf{q}^{N+1}\delta\left(\sum_{i=1}^{N}c_i\mathbf{q}_i-\mathbf{R}_0\right)\psi_{\mathrm{eq}}(\mathbf{q}^{N+1})=1. \tag{3.16}$$

With the expression for $\psi_{\mathrm{eq}}(\mathbf{q}^{N+1})$ in Eq. (3.15), we have

$$\mathcal{N}^{-1}=\left(\pi\sum_{i=1}^{N} c_i^2/\alpha_i\right)^{-3/2}\exp\left(-R_0^2/\sum_{i=1}^{N} c_i^2/\alpha_i\right)=P_O^{\mathrm{eq}}(R_0). \tag{3.17}$$

Next, we introduce an intermediate Green's function,

$$\mathcal{G}_{R_0}(\mathbf{q}^{N+1},t|\mathbf{R}_0)\equiv\mathcal{N}\int d\mathbf{q}_0^{N+1}\mathcal{G}_F(\mathbf{q}^{N+1},t|\mathbf{q}_0^{N+1})\times\delta\left(\sum_{j=1}^{N} c_j\mathbf{q}_{j0}-\mathbf{R}_0\right)\psi_{\mathrm{eq}}(\mathbf{q}_0^{N+1}). \tag{3.18}$$

This is the probability density that the chain conformation at time t is given by $\mathbf{q}^{N+1}$, provided that the relative position vector $\mathbf{R}=\mathbf{r}_i-\mathbf{r}_j$ is $\mathbf{R}_0$ at $t=0$. $G(\mathbf{R},t|\mathbf{R}_0)$ is related to $\mathcal{G}_{R_0}(\mathbf{q}^{N+1},t|\mathbf{R}_0)$ as

$$G(\mathbf{R},t|\mathbf{R}_0)=\int d\mathbf{q}^{N+1}\delta\left(\sum_{i=1}^{N} c_i\mathbf{q}_i-\mathbf{R}\right)\mathcal{G}_{R_0}(\mathbf{q}^{N+1},t|\mathbf{R}_0). \tag{3.19}$$

Since $\mathcal{G}_{R_0}(\mathbf{q}^{N+1},t|\mathbf{R}_0)$ is independent of $\mathbf{q}_0$, we define another auxiliary function by

$$\mathcal{G}_{R_0}(\mathbf{q}^{N+1},t|\mathbf{R}_0)=V^{-1}\mathcal{G}(\mathbf{q}^{N},t|\mathbf{R}_0), \tag{3.20}$$

where $\mathbf{q}^N=(\mathbf{q}_1,\ldots,\mathbf{q}_N)$. Using the Fourier integral representation of the delta-function, we can rewrite Eq. (3.19) as

$$G(\mathbf{R},t|\mathbf{R}_0)=\frac{1}{(2\pi)^3}\int d\mathbf{k}\,e^{i\mathbf{k}\cdot\mathbf{R}}\tilde{\mathcal{G}}(\xi^N,t|\mathbf{R}_0)|_{\xi_i=c_i\mathbf{k}}, \tag{3.21}$$

where $\tilde{\mathcal{G}}(\xi^N,t|\mathbf{R}_0)$ denotes a $3N$-dimensional Fourier transform of $\mathcal{G}(\mathbf{q}^N,t|\mathbf{R}_0)$,

$$\tilde{\mathcal{G}}(\xi^N,t|\mathbf{R}_0)=\int d\mathbf{q}^N\exp\left(-i\sum_{j=1}^{N}\xi_j\cdot\mathbf{q}_j\right)\mathcal{G}(\mathbf{q}^N,t|\mathbf{R}_0) \tag{3.22}$$

with $\xi^N=(\xi_1,\xi_2,\ldots,\xi_N)$ denoting the $3N$ Fourier space variables.

Now our immediate task is to determine $\tilde{\mathcal{G}}(\xi^N,t|\mathbf{R}_0)$. We note that $\mathcal{G}_{R_0}(\mathbf{q}^{N+1},t|\mathbf{R}_0)$ evolves in time according to Eq. (3.11). Since $\mathcal{G}_{R_0}$ is independent of $\mathbf{q}_0$ and $2\nu_0\alpha_0=3\lambda_0/b^2=0$, we obtain

$$\frac{\partial}{\partial t}\mathcal{G}(\mathbf{q}^N,t|\mathbf{R}_0)=D_1\sum_{i=1}^{N}\left[\nu_i\frac{\partial^2\mathcal{G}}{\partial\mathbf{q}_i^2}+2\nu_i\alpha_i\left(\frac{\partial}{\partial\mathbf{q}_i}\right)^T\cdot\mathbf{q}_i\mathcal{G}\right]. \tag{3.23}$$

From Eqs. (3.15) and (3.18), the initial condition for $\mathcal{G}(\mathbf{q}^N,t|\mathbf{R}_0)$ is given by

$$\mathcal{G}(\mathbf{q}^N,t=0|\mathbf{R}_0)=\mathcal{N}\delta\left(\sum_{i=1}^{N} c_i\mathbf{q}_i-\mathbf{R}_0\right)\times\prod_{j=1}^{N}(\alpha_j/\pi)^{3/2}\exp(-\alpha_j\mathbf{q}_j^2). \tag{3.24}$$

Fourier transformations of Eqs. (3.23) and (3.24) give

$$\frac{\partial}{\partial t}\tilde{\mathcal{G}}(\xi^N,t|\mathbf{R}_0)=-D_1\sum_{i=1}^{N}\left[\nu_i\xi_i^2\tilde{\mathcal{G}}+2\nu_i\alpha_i\xi_i^T\cdot\frac{\partial}{\partial\xi_i}\tilde{\mathcal{G}}\right], \tag{3.25}$$

$$\tilde{\mathcal{G}}(\xi^N,0|\mathbf{R}_0)=\exp\left\{-\frac{1}{4}\sum_{i=1}^{N}\frac{\xi_i^2}{\alpha_i}+\left[\frac{1}{4}\left(\sum_{i=1}^{N}\frac{c_i}{\alpha_i}\xi_i\right)^2-i\sum_{i=1}^{N}\frac{c_i}{\alpha_i}\xi_i\cdot\mathbf{R}_0\right]\Big/\left(\sum_{i=1}^{N}\frac{c_i^2}{\alpha_i}\right)\right\}. \tag{3.26}$$

Linear partial differential equations of the type of Eq. (3.25) can be solved by using the Lagrange method of characteristics.[20] After some algebra, we obtain

$$\tilde{\mathcal{G}}(\xi^N,t|\mathbf{R}_0)=\exp\left[-\frac{1}{4}\sum_{i=1}^{N}\frac{\xi_i^2}{\alpha_i}\right]\times\exp\left\{\left[\frac{1}{4}\left(\sum_{i=1}^{N}\frac{c_i}{\alpha_i}\xi_i e^{-2D_1\nu_i\alpha_i t}\right)^2-i\sum_{i=1}^{N}\frac{c_i}{\alpha_i}\mathbf{R}_0\cdot\xi_i e^{-2D_1\nu_i\alpha_i t}\right]\Big/\left(\sum_{i=1}^{N}\frac{c_i^2}{\alpha_i}\right)\right\}. \tag{3.27}$$

From Eqs. (3.21) and (3.27), $G(\mathbf{R},t|\mathbf{R}_0)$ is then given by

$$G(\mathbf{R},t|\mathbf{R}_0)=\left\{\frac{3}{2\pi\langle\mathbf{R}^2\rangle[1-\phi(t)^2]}\right\}^{3/2}\times\exp\left\{-\frac{3[\mathbf{R}-\phi(t)\mathbf{R}_0]^2}{2\langle\mathbf{R}^2\rangle[1-\phi(t)^2]}\right\}, \tag{3.28}$$

where $\mathbf{R}\equiv\mathbf{r}_i-\mathbf{r}_j=\sum_{k=1}^{N}c_k\mathbf{q}_k$. $\langle\mathbf{R}^2\rangle$ denotes the equilibrium mean squared distance between the ith and jth beads, and $\phi(t)$ is the normalized time correlation function of the vector $\mathbf{R}$:

$$\langle\mathbf{R}^2\rangle=b^2\sum_{k=1}^{N}\frac{c_k^2}{\mu_k}=|i-j|b^2, \tag{3.29}$$

$$\phi(t)=\frac{1}{|i-j|}\sum_{k=1}^{N}\frac{c_k^2}{\mu_k}\exp(-3\lambda_k t/t_1), \tag{3.30}$$

where $t_1=b^2/D_1$. The formal structure of the reduced Green's function given by Eq. (3.28) can also be derived by the procedure as suggested by Doi[17] (see the Appendix).

Note that the equilibrium distribution function for the distance R is given by

$$P_o^{\mathrm{eq}}(R)=P_o^{\mathrm{eq}}(\mathbf{R})=\int d\mathbf{q}^{N+1}\delta\left(\sum_{k} c_k\mathbf{q}_k-\mathbf{R}\right)\psi_{\mathrm{eq}}(\mathbf{q}^{N+1})=\left(\frac{3}{2\pi\langle\mathbf{R}^2\rangle}\right)^{3/2}\exp\left(-\frac{3\mathbf{R}^2}{2\langle\mathbf{R}^2\rangle}\right). \tag{3.31}$$

An expression for the orientation-averaged Green's function $G(R,t|R_0)$ can be readily obtained from Eq. (3.28):

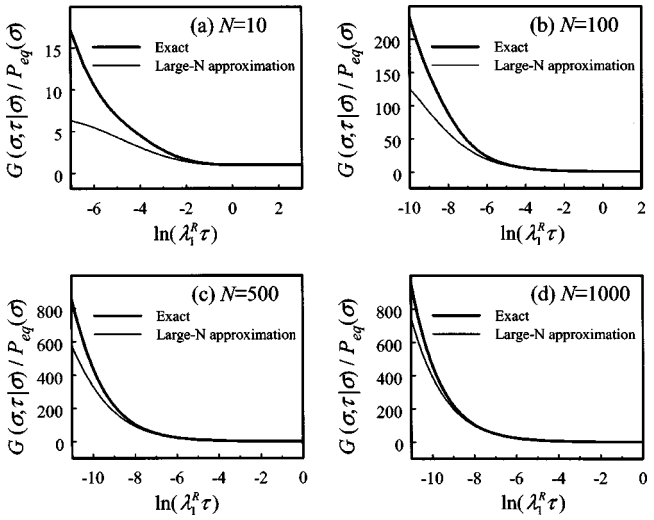

FIG. 2. Accuracy of the large-N approximation for the end-to-end mode Green's function given by Eqs. (3.1) and (3.2). The unit of time is b^2/D_1 and λ_1^R is the relaxation rate of the slowest normal mode of the Rouse chain.

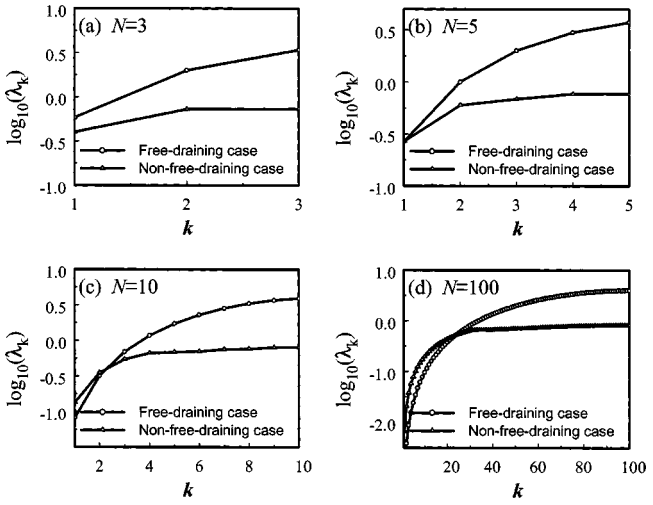

FIG. 3. Effects of hydrodynamic interaction on the relaxation rates of normal modes of the Rouse–Zimm chain.

$$G(R,t|R_0)=\left\{\frac{3}{2\pi\langle\mathbf{R}^2\rangle[1-\phi^2(t)]}\right\}^{1/2}\frac{1}{4\pi RR_0\phi(t)}\times\left\{\exp\left(-\frac{3}{2\langle\mathbf{R}^2\rangle}\frac{[R-\phi(t)R_0]^2}{[1-\phi^2(t)]}\right)-\exp\left(-\frac{3}{2\langle\mathbf{R}^2\rangle}\frac{[R+\phi(t)R_0]^2}{[1-\phi^2(t)]}\right)\right\}. \quad (3.32)$$

For the free-draining Rouse chain, more explicit expressions can be obtained. In this case, we have for $k=0,1,\ldots,N$,

$$\lambda_k^R=\mu_k^R=4\sin^2\left(\frac{k\pi}{2(N+1)}\right),$$
$$c_k^R=-2\left(\frac{2-\delta_{k0}}{N+1}\right)^{1/2}\sin\left[\frac{(i+j+1)k\pi}{2(N+1)}\right]\sin\left[\frac{(i-j)k\pi}{2(N+1)}\right], \quad (3.33)$$

with the superscript R denoting a quantity for the free-draining Rouse chain. In particular, when the reaction occurs between the beads at the chain ends (i.e., $i=0$ and $j=N$), we have $\langle\mathbf{R}^2\rangle=Nb^2$, and the expression for $G(\mathbf{R},t|\mathbf{R}_0)$ reduces to that given by Eqs. (3.1) and (3.3).

IV. DISCUSSION

A. Accuracy of the large-*N* approximation for the Green's function

Most experiments as well as computer simulations on intrachain reactions are carried out for a relatively short polymer that may be modeled as a chain with the number of beads less than 100. Nevertheless, the results are often analyzed by using the approximate expression for the Green's function given by Eqs. (3.1) and (3.2), which is valid only for large values of N.

In Fig. 2, we examine the accuracy of the large-N approximation for $G(R,t|R_0)$ against the exact one given by Eqs. (3.1) and (3.3). For simplicity, our calculations in this section are carried out for the delta-function sink case, which leads to the rather simple expressions for $\hat{S}_R(s)$ as given in Eqs. (2.26) and (2.32). Hence we will examine the value of $G(\sigma,t|\sigma)$ only.

Figure 2(a) shows that the large-N approximation for the Green's function fails badly for a shorter chain with 11 beads ($N=10$). The curve for the approximate result coincides with the exact one only after the Green's function decays to its asymptotic value, $G(\sigma,t|\sigma)/P_O^{\mathrm{eq}}(\sigma)=1$. Even when $N=100$, the large-N approximation fails at short times; see Fig. 2(b). Later, we will see that this short-time deviation produces a considerable error in the calculated reaction rate. As expected, the large N-approximation gets better for longer chains; see Figs. 2(c) and 2(d).

B. Effect of hydrodynamic interaction on the time dependence of the Green's function

To better understand the effect of hydrodynamic interaction (HI) on the time dependence of $G(R,t|R_0)$, we first examine the HI effects on the relaxation rates of normal modes of Rouse–Zimm chains. We assume that the friction coefficient ζ_1 for a single bead is given by $3\pi\eta b$ to calculate the HI matrix given below Eq. (3.6).

Figure 3(a) shows that for a short chain with four beads ($N=3$), the relaxation rates of all normal modes are retarded due to HI. Also for a chain with six beads ($N=5$), the relaxation rates of all normal modes except the slowest one are retarded due to HI; see Fig. 3(b). In this case, the relaxation rate of the slowest normal mode in the presence of HI is about the same magnitude as that in the absence of HI. In contrast, for longer chains with $N=10$ and $N=100$, we can observe a dual influence of HI; see Figs. 3(c) and 3(d). HI retards the high frequency normal modes considerably, but it enhances the relaxation rates of the sluggish normal modes which affect the end-to-end motion of the chain. This behavior can be explained as follows. Since hydrodynamic hindrance retards the relative motion of the neighboring beads, it slows down the relaxation rates of the short wavelength

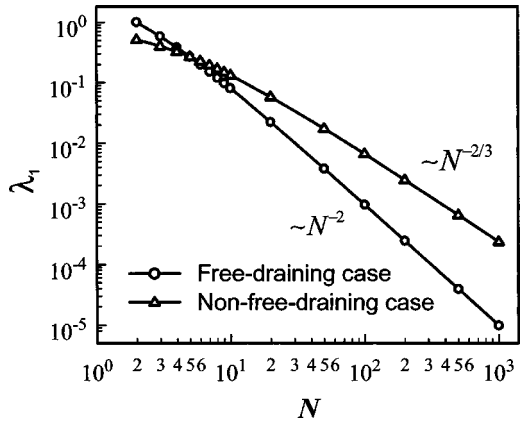

FIG. 4. The relaxation rate λ_1 of the slowest normal mode varying as a function of the bead number.

normal modes. But due to the presence of such hindrance the internal beads are searching the configuration space less compactly, and this can accelerate the long wavelength modes like the end-to-end motion.

The long-time dynamics of the chain are governed by the slowest normal mode. Figure 4 displays the relaxation rate λ_1 of the slowest normal mode varying as a function of the bead number. We see that λ_1 is smaller in the presence of HI for shorter chains with $N<5$, but is larger for longer chains with $N>5$. As is well known, in the free-draining limit λ_1 is inversely proportional to N^2 for large N, while in the presence of HI, it varies as $N^{-3/2}$. [3]

We can now easily understand the effect of HI on the time dependence of $G(\sigma,t|\sigma)$ for end-to-end motion, displayed in Fig. 5. For a short chain with six beads ($N=5$), the Green's function decays more slowly all the time in the presence of HI. However, for a chain with eleven beads ($N=10$), the Green's function decays more slowly only for a short time in the presence of HI. At long times, as the slower normal modes take charge of the behavior of the end-to-end motion, it decays faster in the presence of HI. For a chain

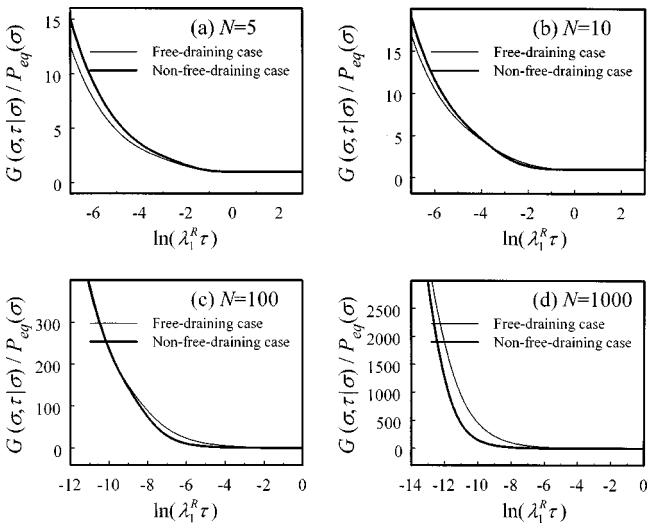

FIG. 5. Effects of hydrodynamic interaction on the time dependence of the end-to-end mode Green's function. The unit of time is b^2/D_1 and λ_1^R is the relaxation rate of the slowest normal mode of the free-draining Rouse chain.

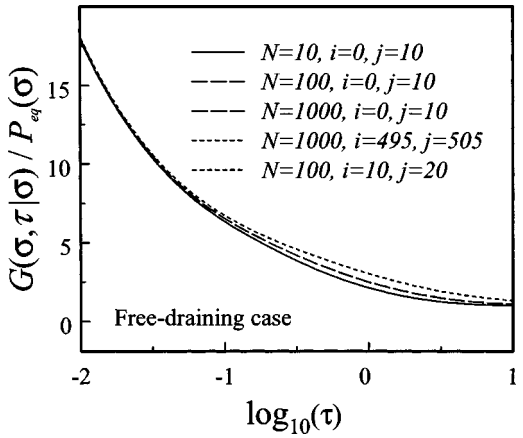

FIG. 6. Variance of the Green's function depending on the reacting group positions, i and j, in the absence of hydrodynamic interaction. In all cases, the reacting groups are separated by ten bonds while the chain length and the positions of reacting groups are varied as indicated in the legend.

with $N=100$, the Green's function decays faster in the presence of HI except at very short times. Figure 5(d) shows that HI drastically enhances the relaxation rate of the end-to-end mode Green's function for a very long chain with $N=1000$. These results show clearly the necessity of the inclusion of HI in considering the intrachain reaction dynamics.

C. Dependence of Green's function on reacting group positions

In Fig. 6 we investigate the dependence of the Green's function on the reacting group positions along the chain backbone. In all cases displayed in Fig. 6 the reacting groups are separated by ten bonds, while the chain length and the positions of reacting groups are varied as indicated in Fig. 6.

We find that the relaxation behaviors of the Green's functions can be grouped topologically into three classes. The first class includes the case where both reacting groups are located at the chain ends, as the one represented by the solid curve ($N=10$, $i=0$, $j=10$). The second class includes the cases where only one of the two reacting groups is located at the chain end as those represented by the dashed curve; the case with $N=100$, $i=0$, and $j=10$ cannot be distinguished from the case with $N=1000$, $i=0$, and $j=10$. The third class includes the cases where both reacting groups are located in the middle of the chain backbone as those represented by the dotted curve; the case with $N=1000$, $i=495$, and $j=505$ cannot be distinguished from the case with $N=100$, $i=10$, and $j=20$.

In the free-draining case, the Green's functions are identical if they belong to the same topological class. This tells us, for example, that the kinetics of reactions between the zeroth and the tenth beads, belonging to the second class, are identical regardless of the chain length.

In the presence of HI, the Green's functions belonging to the same class may differ slightly from one another, but the difference seems to be negligible. It is also interesting that, in the presence of HI, the difference in the Green's functions

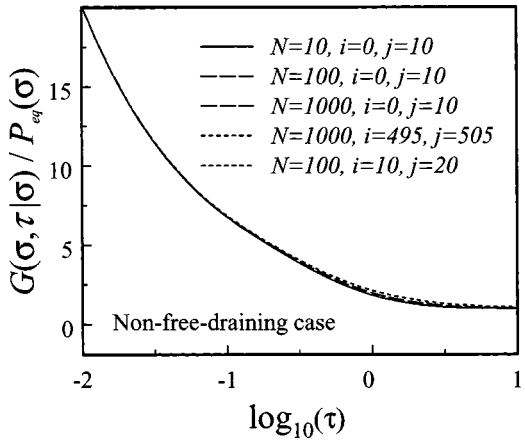

FIG. 7. Variance of the Green's function depending on the reacting group positions, i and j, in the presence of hydrodynamic interaction. In all cases, the reacting groups are separated by ten bonds while the chain length and the positions of reacting groups are varied as indicated in the legend.

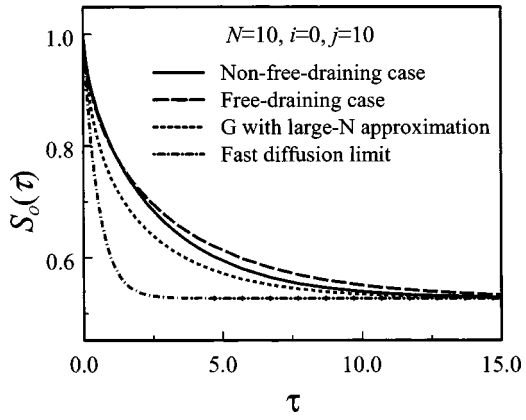

FIG. 9. Time dependence of the probability that the chain polymer is in the open form. The ring-closure reaction occurs between the beads at the chain ends. The reaction parameters used are as follows: $\kappa_f=100$, $k_r^{eq}=1.0$, and $\sigma=1$. The equilibrium probability S_O^{eq} that the chain is in the open form is given by 0.527.

belonging to the different classes becomes smaller, as can be seen from Fig. 7.

D. Kinetics of reversible intrapolymer ring formation

Before investigating the kinetics of intrapolymer excimer-formation reaction, we consider the simpler case of reversible ring formation between reacting groups having infinite lifetimes.

Figure 8 displays the time dependence of the probability that an 11-bead chain is in the open form. The ring-closure reaction occurs between the beads at the chain ends. We have used Eq. (2.32) to calculate $S_O(t)\,[=1-S_R(t)]$. We first calculated $\hat{G}(\sigma,s|\sigma)$ by numerically integrating the time-domain expression of the Green's function given by Eq. (3.32). Then, the result was plugged into the expression for $\hat{S}_R(s)$ to obtain $S_R(t)$ by numerical inverse Laplace transformation. We used the IMSL subroutines DQ2AGS and DINLAP. The parameter values used to calculate the curves in Fig. 8 are as follows: $\kappa_f=10$, $k_r^{eq}=0.1$, and $\sigma=1$. We use dimensionless variables for which the length and time units are b and b^2/D_1, respectively. Hence, the above-given value of k_r^{eq} says that for a time span during which a single bead moves over a distance equivalent to its size, the probability that the ring-form chain will become an open chain is about 0.1. Since $P_O^{eq}(\sigma)=8.98\times10^{-3}$ for the 11-bead chain under consideration, we have $k_f^{eq}=\kappa_f P_O^{eq}(\sigma)=8.98\times10^{-2}$, so that the equilibrium forward rate constant has a similar magnitude to the reverse rate constant, and the equilibrium probability S_O^{eq} that the chain is in the open form is given by 0.527.

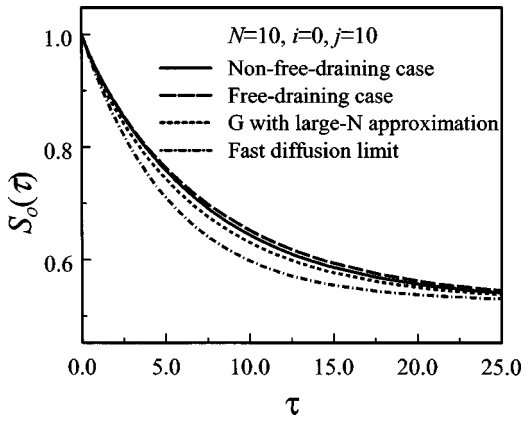

FIG. 8. Time dependence of the probability that the chain polymer is in the open form. The ring-closure reaction occurs between the beads at the chain ends. The reaction parameters used are as follows: $\kappa_f=10$, $k_r^{eq}=0.1$, and $\sigma=1$. The equilibrium probability S_O^{eq} that the chain is in the open form is given by 0.527.

From Fig. 8, we see that except at very short times, the survival probability decays faster in the presence of HI. We also note that if one uses the large-N approximation for the Green's function, it overestimates the relaxation rate of the survival probability to the equilibrium value; the dotted curve should be compared with the dashed curve since the HI effect is not counted in the large-N approximation for the Green's function. However, the differences are not very large in this less diffusion-influenced case. Nevertheless, if one assumes the equilibrium kinetics (the dot-dashed curve), it leads to a considerable error.

Figure 9 shows that the approximate results, especially the large-N approximation and the equilibrium kinetics results, are much worse in the strongly diffusion-influenced case. In this case, the values of the parameters used are $\kappa_f=100$, $k_r^{eq}=1.0$, and $\sigma=1$, so that the equilibrium probability S_O^{eq} is given by the same value of 0.527 as in Fig. 8.

Figure 10 shows that for a longer chain, HI enhances the reaction rate between the end beads to a greater extent. Figure 10 clearly shows the importance of the HI effect in considering the intrachain reactions. The dotted curve calculated by using the large-N approximation for the Green's function still deviates considerably from the dashed curve. The equilibrium kinetics result fails completely. The values of the parameters used are $\kappa_f=1000$, $k_r^{eq}=1.0$, and $\sigma=1$. In this case, $P_O^{eq}(\sigma)=3.25\times10^{-4}$ so that the equilibrium probability S_O^{eq} is given by 0.755.

Figure 11 displays the effect of topological difference in

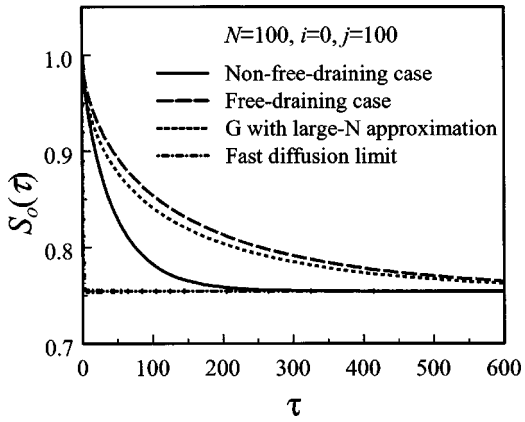

FIG. 10. Time dependence of the probability that the chain polymer is in the open form. The ring-closure reaction occurs between the beads at the chain ends. The reaction parameters used are as follows: $\kappa_f=1000$, $k_r^{eq}=1.0$, and $\sigma=1$. The equilibrium probability S_O^{eq} that the chain is in the open form is given by 0.755.

the reacting group positions on the reaction dynamics. We consider the reactions occurring between the beads that are separated by three bonds. For the case of Fig. 11(a), the reaction occurs between the zeroth and third beads of a 101-bead chain. For the case of Fig. 11(b), the reaction occurs between the beads located in the middle of the chain. In both cases, we have used the following parameters: $\kappa_f=100$, $k_r^{eq}=1.0$, and $\sigma=1$. We also have $P_O^{eq}(\sigma)=3.85\times10^{-2}$ and $S_O^{eq}=0.206$ in both cases. We can see that the reactions occur on the same time scale, but there is a noticeable difference due to the topological difference. In both cases the reactions occur more slowly in the presence of HI at short times. But for the case of Fig. 11(b), there is a crossover in the relaxation curves at an intermediate time, and the reaction proceeds faster in the presence of HI at long times.

E. Kinetics of intrapolymer excimer formation

When the lifetimes of the monomer and excimer are the same ($k_M=k_E=k_S$), the reaction kinetics of excimer formation do not differ much from those of the simple ring closure considered in Sec. IV D. The probability functions $S_O(t)$ and $S_R(t)$ can be obtained just by multiplying the exponential factor $e^{-k_S t}$ to those obtained for the case with $k_S=0$. However, when the lifetimes are different, the time dependencies of $S_O(t)$ and $S_R(t)$ become nontrivial.

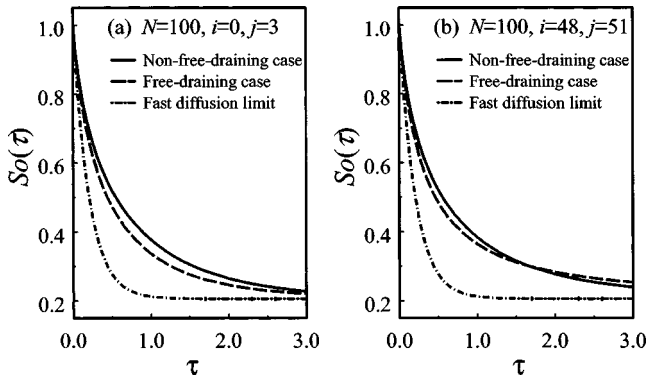

FIG. 11. Time dependence of the probability that the chain polymer is in the open form. The ring-closure reaction occurs between the beads that are separated by three bonds. The reaction occurs between the zeroth and third beads for (a), and between the beads located in the middle of the chain for (b). In both cases, the reaction parameters used are as follows: $\kappa_f=100$, $k_r^{eq}=1.0$, and $\sigma=1$. The equilibrium probability S_O^{eq} that the chain is in the open form is given by 0.206.

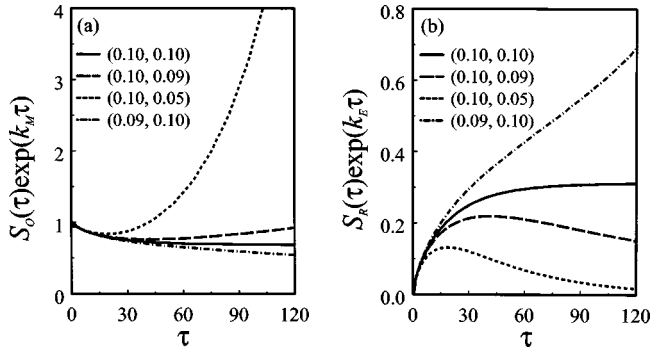

FIG. 12. Time dependence of $S_O(t)$ and $S_R(t)$ in excimer-formation reactions. The number of beads of the chain is 51 ($N=50$), and the excimer-formation reaction occurs between the beads at the chain ends ($i=0, j=50$). Values of other parameters used are $\kappa_f=500$, $k_r^{eq}=1.0$, and $\sigma=1$. The decay rate constants (k_M, k_E) of the monomer and excimer are indicated in the legend.

In Fig. 12, we display how these probability functions behave when there is a disparity in the lifetimes. We have used Eqs. (2.24) and (2.26) to calculate $S_O(t)$ and $S_R(t)$. The number of beads in the chain is 51 ($N=50$), and the excimer-formation reaction occurs between the beads at the chain ends ($i=0, j=50$). Values of other parameters used are $\kappa_f=500$, $k_r^{eq}=1.0$, and $\sigma=1$. The decay rate constants (k_M, k_E) of the monomer and excimer are shown in the legend of Fig. 12. We have $P_O^{eq}(\sigma)=9.06\times10^{-4}$, so that if $k_M=k_E=0$ the equilibrium probability S_O^{eq} would be given by 0.688.

When $k_M=k_E$, the values of $S_O(t)e^{k_M t}$ and $S_R(t)e^{k_E t}$ monotonically converge to their respective asymptotic values, S_O^{eq} and S_R^{eq}. However, when $k_M>k_E$, $S_O(t)e^{k_M t}$ may become much larger than S_O^{eq}, while $S_R(t)e^{k_E t}$ becomes smaller than S_R^{eq}. In the opposite case, the trend is reversed, as can be seen in Fig. 12. The former case has attracted experimentalists' attention because a prolonged fluorescence from the monomer can be observed.

V. CONCLUSION

The key dynamic quantity in the reaction kinetics of intrachain reactions is the Green's function which describes the dynamics of the relative motion of the reacting groups. Based on the Rouse–Zimm model for the chain polymers, we have derived an expression for the Green's function that can be applied to a more general situation where the reacting groups are located at any position of the chain backbone. It also takes into account the effect of hydrodynamic interaction in the pre-averaged form.

We have also presented an improved theory for analyzing the kinetics of reversible excimer-formation reaction occurring in a chain polymer. When the lifetimes of the monomer and excimer are set equal to infinity, the present theory

reduces to that for the simple reversible ring-closure reaction considered by Wilemski and Fixman.[3] The present theory generalizes their result for treating the case with arbitrary reacting group locations.

Various aspects of the reaction kinetics of reversible ring-closure and excimer-formation reactions have been investigated, such as the effect of hydrodynamic interaction and the dependence of reaction rate on the positions of reacting groups as well as on the chain length.

In the present theory, we have neglected the effects of excluded volumes and chain stiffness in considering the nonreactive dynamics of the chain polymer. Generalization of the present theory in this direction is in progress.

ACKNOWLEDGMENTS

This work was supported by Grant No. R03-2001-00022 from the Basic Research Program of the Korea Science & Engineering Foundation and in part by the Center for Molecular Catalysis.

APPENDIX: AN ALTERNATIVE DERIVATION OF THE GREEN'S FUNCTION

Here, we present an alternative derivation of the reduced Green's function (RGF) given by Eq. (3.28). The definition, Eq. (3.13), indicates that the RGF should be Gaussian for R and R_0:

$$G(\mathbf{R},t|\mathbf{R}_0)=N\exp\left\{-\frac{1}{2}[\mathbf{R}\cdot\mathbf{H}_1\cdot\mathbf{R}+2\mathbf{R}\cdot\mathbf{H}_2\cdot\mathbf{R}_0+\mathbf{R}_0\cdot\mathbf{H}_3\cdot\mathbf{R}_0]\right\}, \tag{A1}$$

where N is a normalization constant, and $\mathbf{H}_i\,(i=1,2,3)$ is a time-dependent matrix. For an isotropic system, $G(\mathbf{R},t|\mathbf{R}_0)$ depends on the magnitudes of $\mathbf{R}$ and $\mathbf{R}_0$ and on the relative angle between $\mathbf{R}$ and $\mathbf{R}_0$, but is independent of the respective orientations of $\mathbf{R}_0$ and $\mathbf{R}$ in the laboratory fixed frame. Hence, $\mathbf{H}_i$ must be proportional to unit matrix, i.e., $\mathbf{H}_i=h_i(t)\mathbf{I}$.

In addition, the RGF satisfies the following properties:

$$\int d\mathbf{R}\,G(\mathbf{R},t|\mathbf{R}_0)=1, \tag{A2}$$

$$\int d\mathbf{R}_0 G(\mathbf{R},t|\mathbf{R}_0)P_O^{\mathrm{eq}}(\mathbf{R}_0)=P_O^{\mathrm{eq}}(\mathbf{R}), \tag{A3}$$

where $P_O^{\mathrm{eq}}(\mathbf{R})$ is the equilibrium distribution. From Eq. (A2), we can show that $N=(h_1/2\pi)^{3/2}$ and $h_2^2=h_1h_3$, so that Eq. (A1) becomes

$$G(\mathbf{R},t|\mathbf{R}_0)=\left(\frac{h_1}{2\pi}\right)^{3/2}\exp\left\{-\frac{h_1}{2}[\mathbf{R}+h_2\mathbf{R}_0/h_1]^2\right\}. \tag{A4}$$

At long times, we must have $h_1(\infty)=3/\langle\mathbf{R}^2\rangle\equiv h_1^\infty$ and $h_2(\infty)=0$, since $\lim_{t\to\infty}G(\mathbf{R},t|\mathbf{R}_0)=P_O^{\mathrm{eq}}(\mathbf{R})$ and $\langle\mathbf{R}^2\rangle=\int d\mathbf{R}\,\mathbf{R}^2P_O^{\mathrm{eq}}(\mathbf{R})$.

From Eq. (A3), we can obtain $h_1=h_1^\infty/(1-y)^2$ with $y=-h_2/h_1$, and Eq. (A4) becomes

$$G(\mathbf{R},t|\mathbf{R}_0)=\left(\frac{3}{2\pi\langle\mathbf{R}^2\rangle(1-y)^2}\right)^{3/2}\times\exp\left\{-\frac{3[\mathbf{R}-y\mathbf{R}_0]^2}{2\langle\mathbf{R}^2\rangle(1-y)^2}\right\}. \tag{A5}$$

Finally, y can be related to $\langle\mathbf{R}(t)\cdot\mathbf{R}(0)\rangle$ by

$$\langle\mathbf{R}(t)\cdot\mathbf{R}(0)\rangle=\int d\mathbf{R}\int d\mathbf{R}_0\mathbf{R}\cdot\mathbf{R}_0G(\mathbf{R},t|\mathbf{R}_0)P_O^{\mathrm{eq}}(\mathbf{R}_0)=y\langle\mathbf{R}^2\rangle, \tag{A6}$$

and we can show that the quantity $y=\langle\mathbf{R}(t)\cdot\mathbf{R}(0)\rangle/\langle\mathbf{R}^2\rangle$ is given by the expression in Eq. (3.30) for the Rouse–Zimm chain.

[1] M. A. Winnik, Acc. Chem. Res. **18**, 73 (1985).
[2] A. T. Reis e Sousa, E. M. S. Castanheira, A. Fedorov, and J. M. G. Martinho, J. Phys. Chem. A **102**, 6406 (1998).
[3] G. Wilemski and M. Fixman, J. Chem. Phys. **60**, 866 (1974); **60**, 878 (1974).
[4] M. Doi, Chem. Phys. **11**, 107 (1975); S. Sunagawa and M. Doi, Polym. J. (Tokyo) **8**, 239 (1975).
[5] M. Battezzati and A. Perico, J. Chem. Phys. **74**, 4527 (1981); **75**, 886 (1981).
[6] G. H. Weiss, J. Chem. Phys. **80**, 2880 (1984).
[7] K. Seki, A. V. Barzykin, and M. Tachiya, J. Chem. Phys. **110**, 7639 (1999).
[8] R. W. Pastor, R. Zwanzig, and A. Szabo, J. Chem. Phys. **105**, 3878 (1996).
[9] G. Srinivas, A. Yethiraj, and B. Bagchi, J. Chem. Phys. **114**, 9170 (2001); G. Srinivas, K. L. Sebastian, and B. Bagchi, *ibid.* **116**, 7276 (2002).
[10] A. V. Barzykin, K. Seki, and M. Tachiya, J. Chem. Phys. **117**, 1377 (2002).
[11] B. Friedman and B. O'Shaughnessy, Phys. Rev. A **40**, 5950 (1989); Europhys. Lett. **21**, 779 (1993).
[12] J. Stampe and I. M. Sokolov, J. Chem. Phys. **114**, 5043 (2001).
[13] A. Dua and B. J. Cherayil, J. Chem. Phys. **116**, 399 (2002).
[14] T. Bandyopadhyay and S. K. Ghosh, J. Chem. Phys. **116**, 4366 (2002).
[15] A. Rey and J. J. Freire, Macromolecules **24**, 4673 (1991).
[16] A. Podtelezhnikov and A. Vologodskii, Macromolecules **30**, 6668 (1997).
[17] M. Doi, Chem. Phys. **9**, 455 (1975).
[18] J. Sung and S. Lee, J. Chem. Phys. **115**, 9050 (2001).
[19] P. E. Rouse, J. Chem. Phys. **21**, 1272 (1953); B. H. Zimm, *ibid.* **24**, 269 (1956).
[20] E. Zauderer, *Partial Differential Equations of Applied Mathematics* (Wiley, New York, 1983).